AFRL-RH-BR-TR-2007-0078

Effects of Facial Topography and Eyewear on the 94 GHz Beam

Naval Health Research Center Detachment
Directed Energy Bioeffects Division

Donald Hatcher
Donald Marchello
Duane Cox
John D'Andrea
John Ziriax

Air Force Research Laboratory
Directed Energy Bioeffects Division

Leland Johnson
Charles Kuhnel

Nov 2007

Air Force Research Laboratory
Human Effectiveness Directorate
Directed Energy Bioeffects Division
Radio Frequency Radiation Branch
Brooks-City-Base TX 78235

Notice Page for Unlimited Distribution Report Approved for Public Release

NOTICE AND SIGNATURE PAGE

Using Government drawings, specifications, or other data included in this document for any purpose other than Government procurement does not in any way obligate the U.S. Government. The fact that the Government formulated or supplied the drawings, specifications, or other data does not license the holder or any other person or corporation; or convey any rights or permission to manufacture, use, or sell any patented invention that may relate to them.

This report was cleared for public release by the Air Force Research Laboratory, Brooks City-Base, Public Affairs Office and is available to the general public, including foreign nationals. Copies may be obtained from the Defense Technical Information Center (DTIC) (http://www.dtic.mil).

AFRL-RH-BR-TR-2007-0078 HAS BEEN REVIEWED AND IS APPROVED FOR PUBLICATION IN ACCORDANCE WITH ASSIGNED DISTRIBUTION STATEMENT.

_____//SIGNED//_____
NOEL D. MONTGOMERY, LtCol, USAF
Work Unit Monitor

_____//SIGNED//____
GARRETT D. POLHAMUS, DR-IV, DAF
Chief, Directed Energy Bioeffects Division

This report is published in the interest of scientific and technical information exchange, and its publication does not constitute the Government's approval or disapproval of its ideas or findings.

REPORT DOCUMENTATION PAGE

Form Approved
OMB No. 0704-0188

1. REPORT DATE *(DD-MM-YYYY)*	**2. REPORT TYPE**	
29-11-2005	FINAL TECHNICAL REPORT	2004-2005

4. TITLE AND SUBTITLE
Effects of Facial Topography and Eyewear on the 94 GHz Beam

5a. CONTRACT NUMBER
AFRL – 0367 AFRL 00003

5b. GRANT NUMBER

5c. PROGRAM ELEMENT NUMBER

6. AUTHOR(S)
Donald Hatcher, Donald Marchello, Duane Cox, John D'Andrea, John Ziriax, Leland Johnson, Charles Kuhnel

5d. PROJECT NUMBER
7757

5e. TASK NUMBER
B3

5f. WORK UNIT NUMBER
48

7. PERFORMING ORGANIZATION NAME(S) AND ADDRESS(ES)

Naval Health Research Center
Detachment 8315 Navy Road
Brooks City-Base, TX 78235

8. PERFORMING ORGANIZATION REPORT NUMBER

DEBL-2005-03

9. SPONSORING / MONITORING AGENCY NAME(S) AND ADDRESS(ES)
Air Force Materiel Command
Human Effectiveness Directorate
Directed Energy Bioeffects Division
Brooks City Base, TX 78235

10. SPONSOR/MONITOR'S ACRONYM(S)
AFRL/RHD

11. SPONSOR/MONITOR'S REPORT NUMBER(S)
AFRL-RH-BR-TR-2007-0078

12. DISTRIBUTION / AVAILABILITY STATEMENT
Distribution Unlimited, Distribution A- approved for Public Release, Public Affairs Case File No. 07-405, 7 December 2007.

13. SUPPLEMENTARY NOTES
See JNLWD Approval

14. ABSTRACT

15. SUBJECT TERMS
94 GHz, ADS, eyewear , phantom, tissue equivalent material

16. SECURITY CLASSIFICATION OF:			**17. LIMITATION OF ABSTRACT**	**18. NUMBER OF PAGES**	**19a. NAME OF RESPONSIBLE PERSON**
a. REPORT	**b. ABSTRACT**	**c. THIS PAGE**			Lt Col Noel Montgomery
Unclassified	Unclassified	Unclassified	SAR	22	**19b. TELEPHONE NUMBER** *(include area code)*

Standard Form 298 (Rev. 8-98)
Prescribed by ANSI Std. Z39.18

This page intentionally left blank

TABLE OF CONTENTS

Executive Summary

Background

Recently, a millimeter wave (MMW) hardware system, called Active Denial System (ADS) has been developed for use as a non-lethal weapon system. The ADS system is capable of generating high power MMWs and is to be used for, but not limited to, crowd management and denying access to restricted areas. ADS achieves this end by using a 94 GHz MMW beam to produce rapid skin heating to a temperature that causes intense discomfort in a very short period of time, normally in just a matter of seconds. The intensity of the discomforting sensation rapidly decreases when the power to the transmitter is turned off or the individual moves out of the MMW beam. The primary effect of the ADS is heating of skin and absorption of the 94GHz millimeter waves in the eye. Recently the effects that eyewear may have on the absorption of 94 GHz MMWs on the face have been questioned.

Objective

To fully understand the effects of ADS through eyewear, exposure data must be collected while the targeted subject is wearing various types of eyewear, such as, eyeglasses, night vision goggles (NVG) and binoculars, that may be encountered when subjects are be exposed to the system. This investigation was conducted to evaluate the effects that various types of eyewear may have on absorption of the 94 GHz beam and especially the production of hotspots generated by reflections or focusing of the beam on the surface of the face.

Approach

Phantom faces, made of a gel material poured into plastic molds, were used in this study. The face molds were made from moldable plastic heated in an oven, placed over a life form mask, and vacuum formed to create a life-like facial structure. The molds were then used to cast phantom faces out of muscle simulating gel material. The 94GHz exposures caused rapid heating on the surface of the phantom tissue from baseline temperatures of ~22° to as high as 32°. Exposures were conducted with the 94 GHz beam at different angles relative to the face. Thermal data was collected using an infrared camera (FLIR S-60) and evaluated using software (ThermaCAM Researcher Pro 2.7) to determine if thermal hotspots were produced by any of the eyewear placed on the face molds.

Results

Evaluations show that all face shapes absorb and scatter MMWs somewhat differently, due mainly to the shape and size of the nose. However, temperature rise in all cases are very similar with no single exposure elevating to a level more that 10-degrees above pre-exposure values. Not one of the face shapes that were exposed showed any distinct focusing of the beam or hotspots caused by deflection of the beam any more than other shapes that were compared. When wearing no eyewear, it was observed that in all cases the highest temperature increase was located in the inner canthus area of the eye of the phantom face. Heating of the phantom and human faces were compared following exposure to the 94 Ghz beam at an energy level of 1.4 J/cm². IR images from the Flir S-60 were used to evaluate the heating and indicate that the two different types of targets, four phantom and four human, effect the beam in the same manner creating striations caused by the deflection of the beam.

When wearing NVGs and binoculars, the hottest spots on the phantom faces were located outside the area of the eye, normally on the forehead or nose area.

Conclusions

The effect of eyewear on the pattern of absorption of the 94GHz beam has been described. Infrared data showed that there was no unusual heating of the surface around the eye or face due to the eyewear and there is no indication that the NVGs or binoculars focus the beam towards the area of the eye. This data will be used to determine safe operating exposures to the ADS. In a real life situation, a subject would attempt to escape from the MMW beam before any damaging heating could occur.

Abstract

The purpose of the study reported here was to observe the effects of eyewear on absorption of the 94 GHz beam. Four different muscle equivalent tissue real-life face molds were exposed to 94GHz radiation at a fluence of 1.4 J/cm². Surface temperature was measured using an infrared camera (FLIR, Model S-60) during each exposure. The angle of incidence was changed between each exposure to evaluate the effects of the eyewear from varying directions of irradiation. Temperature rise (ΔT) in degrees centigrade (°C) was used to evaluate heating on the surface of the phantom face to determine hotspots that occurred as well as the lack of heating on some areas of the face, including those areas directly behind the eyewear.

Introduction

The radio frequency (RF) portion of the electromagnetic spectrum includes electromagnetic waves with frequencies in the range of 3 kHz to 300 GHz. The MMW frequency range is a subset within the RF region of the spectrum, comprising the frequency range from 30 to 300 GHz. Recently, millimeter wave (MMW) hardware, called the Active Denial System (ADS), has been developed for use as a non-lethal weapon. ADS uses a 94 GHz MMW beam to prevent an individual or group of individuals from advancing or entering controlled locations. Because the beam is traveling at the speed of light, the energy from the beam quickly reaches the subject, penetrates less than 0.3 mm into the skin, and rapidly heats up the surface of the skin. The ADS was designed to produce this rapid heating of the skin to produce intense discomfort. The discomfort is alleviated when the power is turned off or the natural reaction of the subject to escape the beam. The primary effect of the ADS is heating of skin and eyes. MMW absorption and skin/eye heating will occur at a rate determined by the power density at the surface of the tissue and the amount of energy reflected. The higher the power density, the faster the heating which, in turn, will cause the intensity of discomfort to be felt more quickly. Eyewear may cause reflections off metal surfaces and focal hotspots which could produce greater than intended heating. The purpose of this study was to evaluate the possibility of hotspots produced by eyewear such as eyeglasses, NVGs, and binoculars.

Materials and Methods

Subjects - Tissue equivalent material face molds were created from life-masks purchased at Haunted Studios, Incorporated (San Francisco, CA). Four different face molds were selected which provided a variety of facial structures. To examine the effects on the 94GHz beam, three different types of eyewear were selected: eyeglasses, binoculars (Nikon Model00008), and night vision goggles (AN/PVS-7D). All three types of eyewear were placed individually on the face in a position that generally represented the normal wearing of the different eyewear.

Apparatus

Millimeter Wave Exposure System - The exposure facility consisted of a 20’ X 30’ anechoic chamber. Inside the anechoic chamber a smaller 12’ X 12’ Styrofoam® environmentally controlled room provided consistent temperature and humidity control. Exposure to energy density of 1.4 J/cm^2 was performed using a MMW exposure system in a far field exposure facility based on a coupled cavity traveling wave tube amplifier with an output of 800 W (North Star Research Corporation). The exposure setup consisted of 94 GHz standard gain horn with a built-in waveguide window to allow waveguide pressurization with SF6 gas.

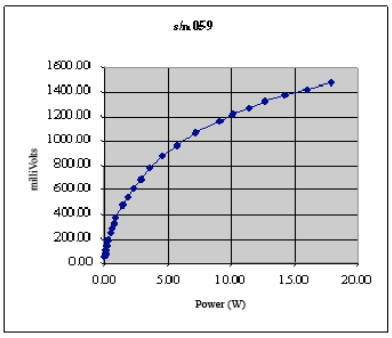

Figure 1. Calibration of the crystal detector (mV) used to measure field power density

Measurements of field power density were done at 250-cm from the horn using a crystal detector (Millitech DXP-08). The following technique was used to measure the power density in the exposure field. The initial step was to standardize the crystal detector by measuring the output voltage as compared to the input power. The output of the detector is non-linear, so numerous steps are measured across the range of the detector from threshold to saturation. The calibration results are plotted and shown in Figure 1. The crystal detector was mounted on a three-axis precision manipulator for accurate scanning (millimeter resolution). The crystal detector was unable to handle 100% of the power at the point of interest so additional attenuation was required to protect the detector. The in-field measuring probe consisted of: 1) Crystal Detector, 2) 20.82 dB attenuator, 3) 11.24 dB 10W attenuator, and 4) Open Ended waveguide 16cm long (13.01 dB of attenuation). The initial step of power measurement was to locate the center of the beam. Using an IR camera and carbon coated Teflon sheet, the beam was located and marked on the IR camera's monitor. The Teflon was removed and the detector and 3-axis manipulator stand was placed in the field and aligned using the IR equipment. The transmitter was set to operate at 1Hz and energized. Using the 3-axis manipulator the probe was adjusted vertically and horizontally until the peak voltage out was indicated thus showing the center of the beam.

Surface Temperature Measurements - A Flir System Model S60 infrared camera (Flir Systems, Boston, MA) was used to collect the temperature data. ThermaCAM Researcher 2.7 IR software was used to control the camera and acquire image data. The IR camera was set to collect data at a rate of 60 frames per second. The software described above was used to measure temperature of the IR images. An external calibration for the Flir S-60 camera was performed using a black-body source (Mikron, Model M340, Mikron Instrument Company, Inc., 16 Thornton Road, Oakland, NJ 07436). Most images were collected with the camera placed on a tripod to one side of the feed horn at an angle that allowed the most direct and unobstructed view of the face model during exposures.

Procedures

The procedure for determining the effects eyewear, such as binoculars, glasses, and night-vision goggles, at a frequency of 94 GHz is described. Data obtained from this procedure was used to determine the heating patterns on the face formed by the deflected 94 GHz beam. During this experiment, four different face shapes were investigated. Each of the face molds that were selected had a unique feature (nose, eye socket, etc...) to show a comparison of effects to these dissimilar facial shapes (see Figure 2).

Figure 2. Real life face molds (left to right: Karloff, Jolie, Hoffman, Lugosi)

For this experiment, face molds were made from moldable plastic heated in an oven, placed over a life form mask, and vacuum formed. The face molds were fastened to a PVC sheet that had PVC rods protruding outward to form a cage-like apparatus to assist in holding the phantom mixture in place once it gelled (see Figure 3). The molds were filled with a mixture of a gelling agent (TX-150), polyethylene powder, salt, and water. This mixture is similar to the simulated phantom muscle material

Figure 3. Mask form holder constructed from PVC

described in the Radio Frequency Radiation Dosimetry Handbook, Fourth Edition. Because there are no formulas for mixing the phantom muscle for 94GHz, the formula for 2450 MHz was used. However, to allow the mixture to retain its shape for a longer period of time, the amount of gelling agent (TX-150) was increased by 1%.

The phantom faces were then exposed to 94GHz MMWs 250-cm in front of the pyramidal horn antenna with sufficient power density and duration of exposure to produce 1.4 J/cm^2. At this distance the beam covered most of the face and included the area of interest around the eyes. Each of the four phantom faces was exposed with and without the eye glasses, binoculars, and NVGs (see Figure 4). Sequences of IR images were taken during the exposures using the FLIR S-60 infrared camera. Temperature across each face image was determined and temperature rise and decay plotted. The images were searched by the software and the area of peak heating was determined. This was deemed the hotspot on the face and compared to heating with and without the different eyewear to evaluate effect of the eyewear on the hotspot or generation of new hotspots. The exposures were done at angles of 0°, 15° and 45° left and right of the horizontal plane and angles of 0°, 15° and 45° above and below the vertical plane.

Figure 4. Phantom face model with various eyewear

Results

Phantom-to-Human Comparison

Four phantom face models exposed to 94GHz at a power of 1.4 J/cm² were compared to four humans exposed to the same levels. The data for the human exposures was collected and conducted in compliance with all applicable federal regulations governing the protection of human subjects in research under Air Force protocol F-WR-2002-0023-H and is reported in NHRC-DET DEBL Technical Report 2005-05: "Threshold of Human Aversion to Brief 94GHz Exposure". In the human study, eyewear was not tested, therefore, only the exposures with no eyewear on the phantom faces were selected for comparison. In every case, whether phantom or human, the hottest points on the face occur in the inner canthus area of the eye. In addition, striations occur on all eight subjects (human and phantom) and are similar in shape and position on the face (Figure 5).

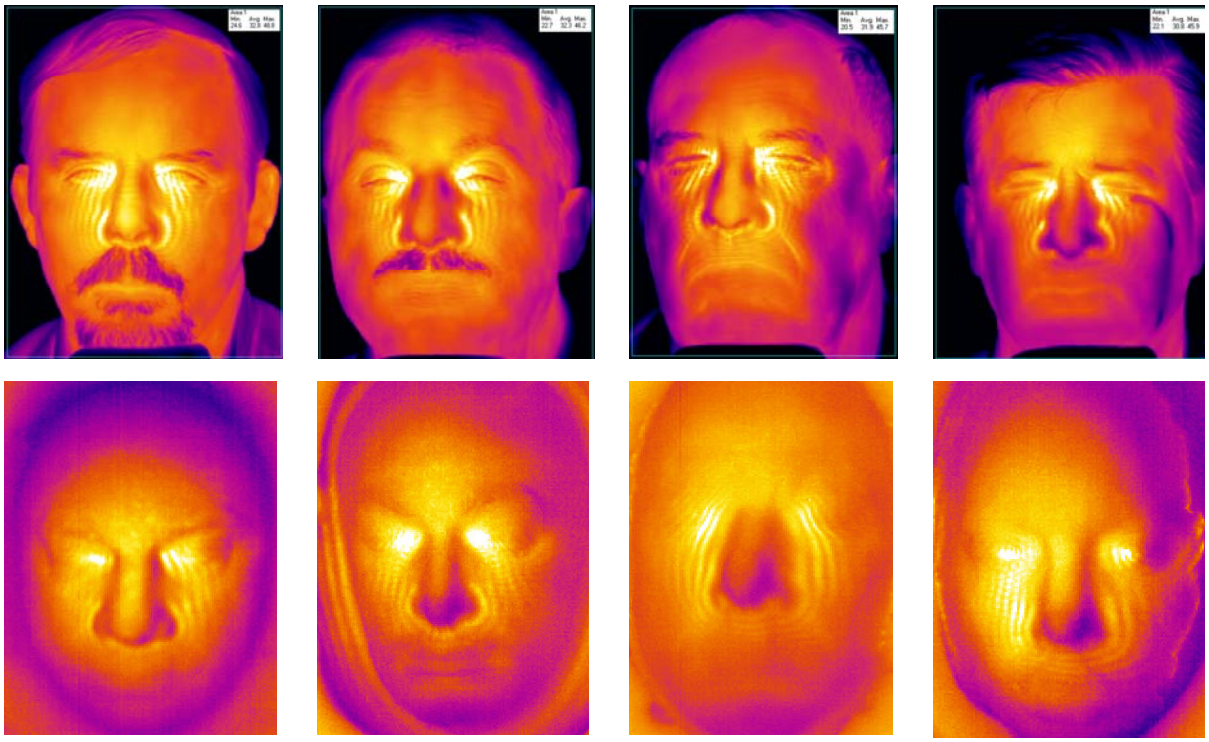

Figure 5. Comparison of phantom and human face heating after being exposed to 94 GHz at an energy level of 1.4 J/cm²

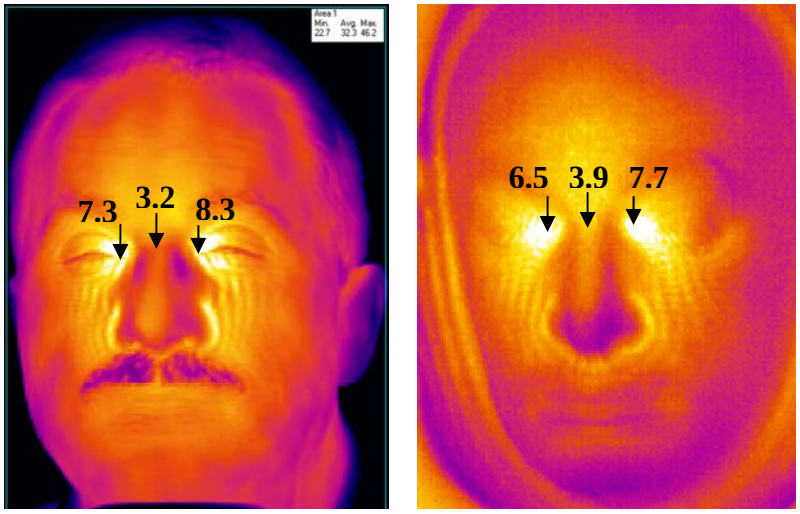

Figure 6. Example of one Human Subject-to-Phantom face comparison of heating in the inner canthus and nose area of the eye.

Human-to-Phantom temperature comparisons were made and clearly illustrate the similarity of millimeter wave absorption (Fig. 6). In every case, both human and phantom exposures produced similar temperature increases in the same areas surrounding the eyes and nose. As with the human subjects, absorption in the phantom face models varied dependent upon the structural shape of the face. To further illustrate the human-to-phantom comparison, temperature changes (ΔT) for three locations (left inner canthus, nose, and right inner canthus) were recorded from seven human subjects and four phantom faces (Figure 7).

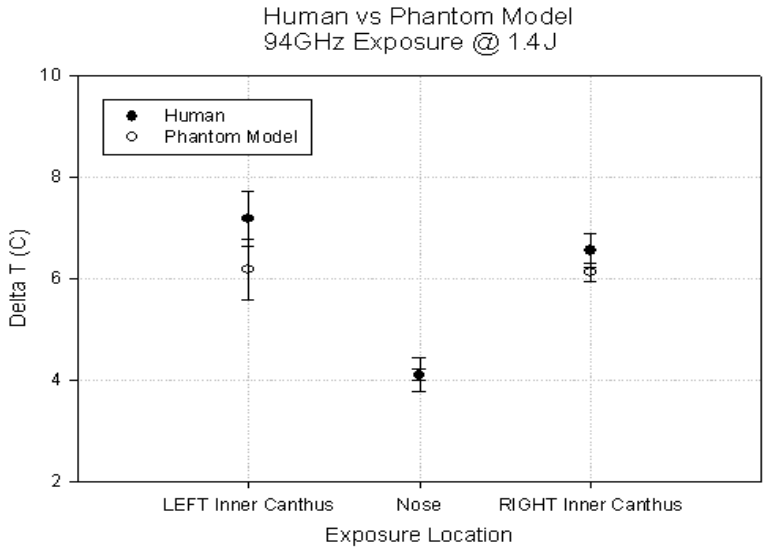

Figure 7. Human vs Phantom Model

No Eyewear

To evaluate the effects of eyewear on the 94GHz beam, infrared pictures were converted to color-coded images using a Microsoft Excel macro (ModelColorCoder.xls, Hatcher, 2000) that assigns a color to the temperature data and places that color as well as the temperature value in each cell of the spreadsheet. A pre-exposure image and an image taken at the time the transmitter was turned off were used to create a subtraction file. This file was used to show the temperature differences between the pre- and post-exposure images to reflect the hottest areas of temperature rise. Figure 8 illustrates the temperature changes on the phantom face with no eyewear. Figure 9 is a graph of the temperature rise located at the hottest spot on the surface of the face.

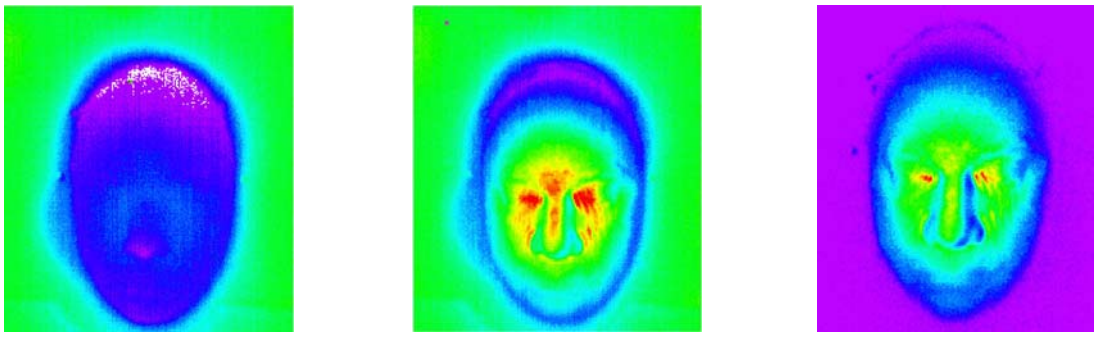

Figure 8. Effects of 94GHz on the phantom face (Lugosi) wearing no eyewear. Left to right: pre-exposure, post-exposure, and difference files

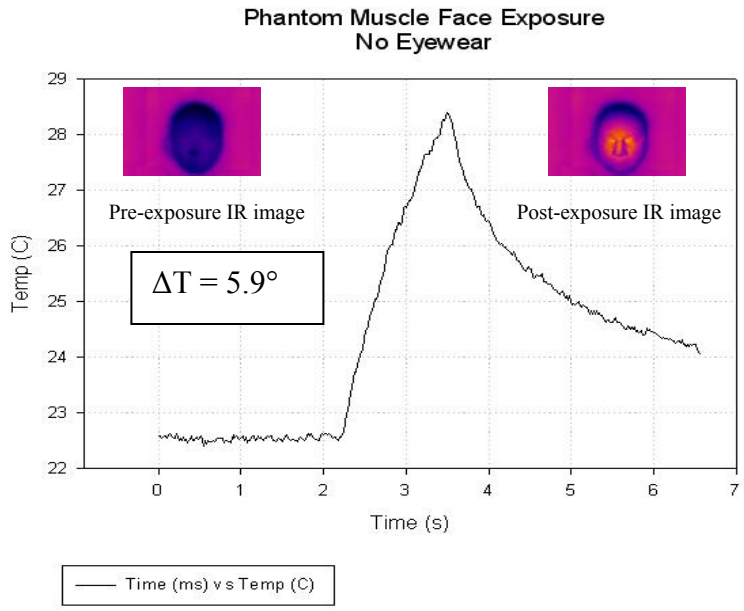

Figure 9. Temperature (C) rise during exposure as recorded by the FLIR S-60 infrared camera.

Eyeglasses

Effects were also examined using eyeglasses (Fig. 10). As with the images recorded with no eyewear, pre, post and difference files were recorded. Figure 11 shows the temperature rise at the hottest spot on the face during exposure.

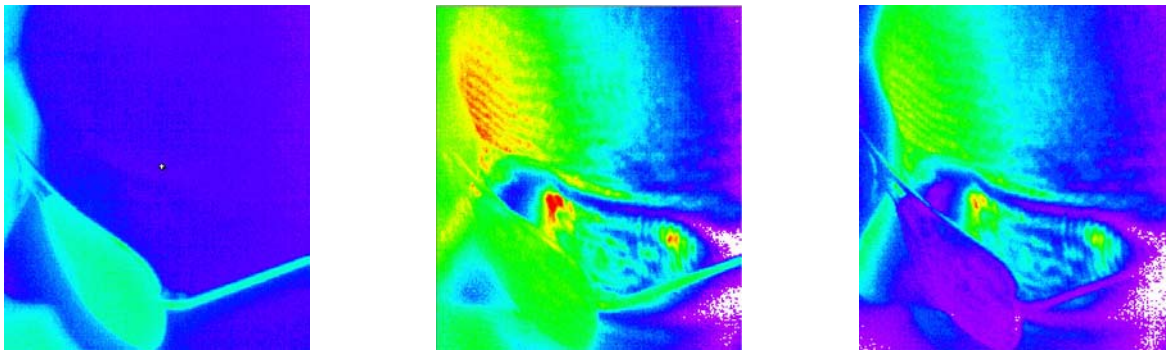

Figure 10. Effects of 94GHz on the phantom face (Lugosi) wearing eye glasses. Left to right: pre-exposure, post-exposure, and difference files

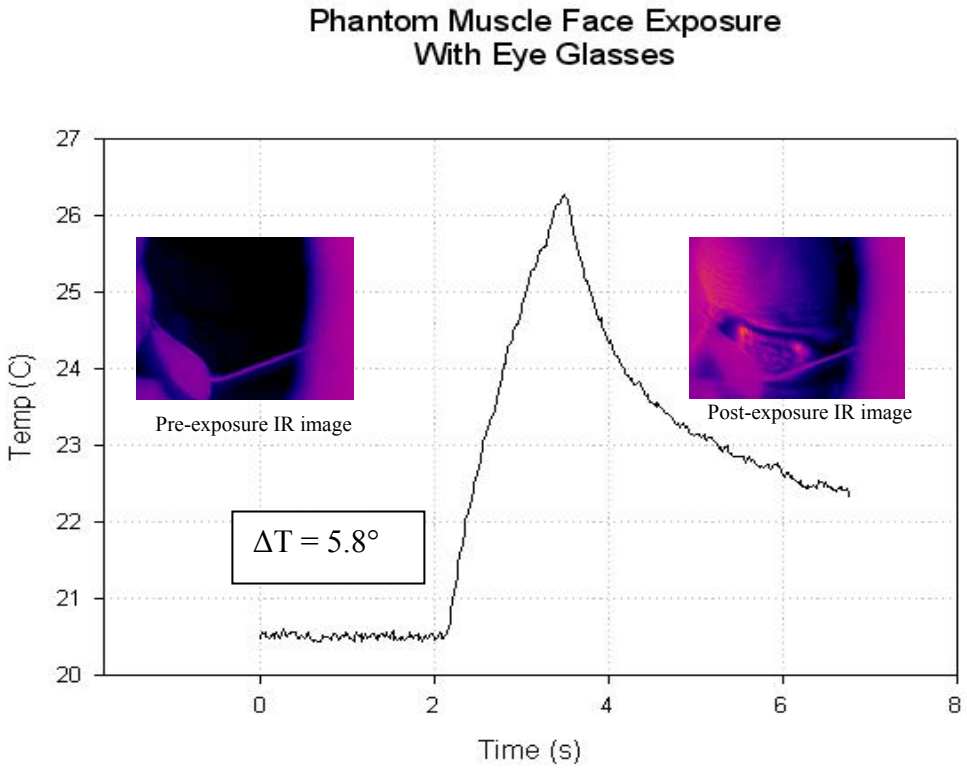

Figure 11. Temperature (C) rise on face (not eye glasses) during exposure as recorded by the FLIR S-60 infrared camera.

Night Vision Goggles and Binoculars

Figure 12 and 14 show the same results when the phantom face is wearing night vision goggles AN/PVS-7D) and binoculars (Nikon 100008), respectively. Figure 13 and 15 illustrate the temperature rise during exposure of the hottest spot.

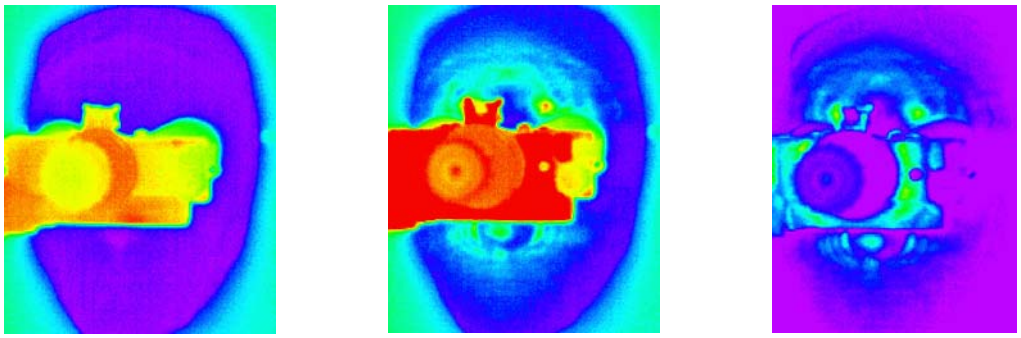

Figure 12. Effects of 94GHz on the phantom face (Lugosi) wearing night vision goggles. Left to right: pre-exposure, post-exposure, and difference files

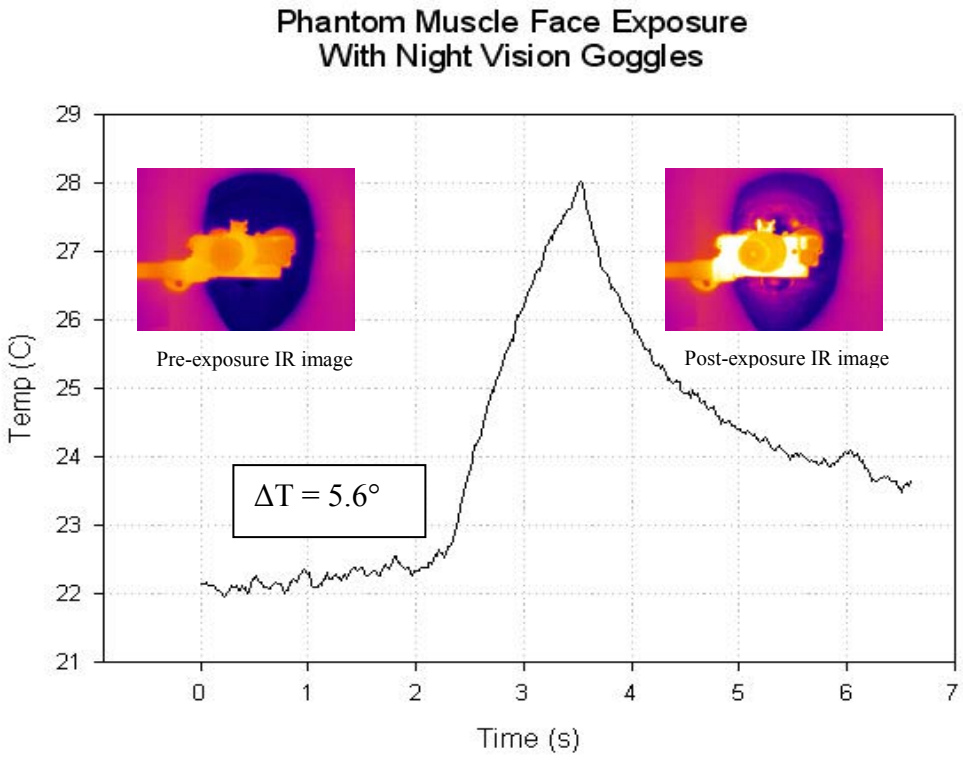

Figure 13. Temperature (C) rise on face (not NVGs) during exposure as recorded by the FLIR S-60 infrared camera.

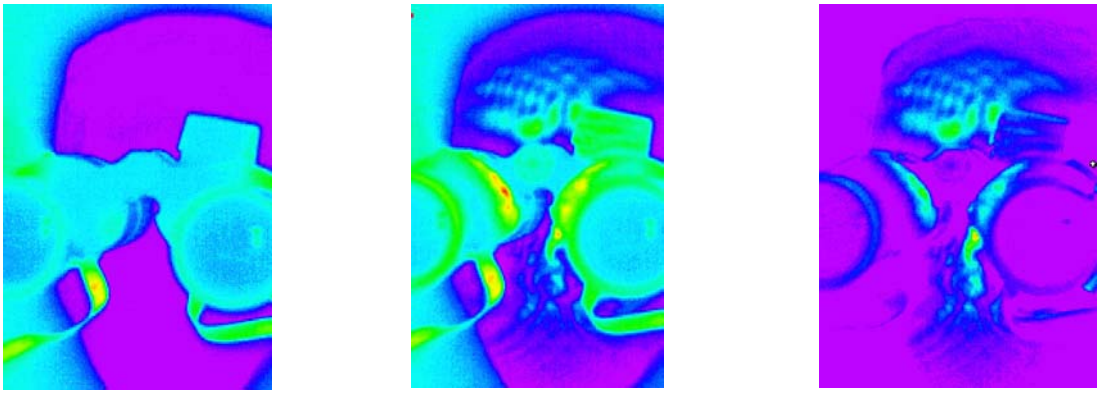

Figure 14. Effects of 94GHz on the phantom face wearing binoculars. Left to right: pre-exposure, post-exposure, and difference files

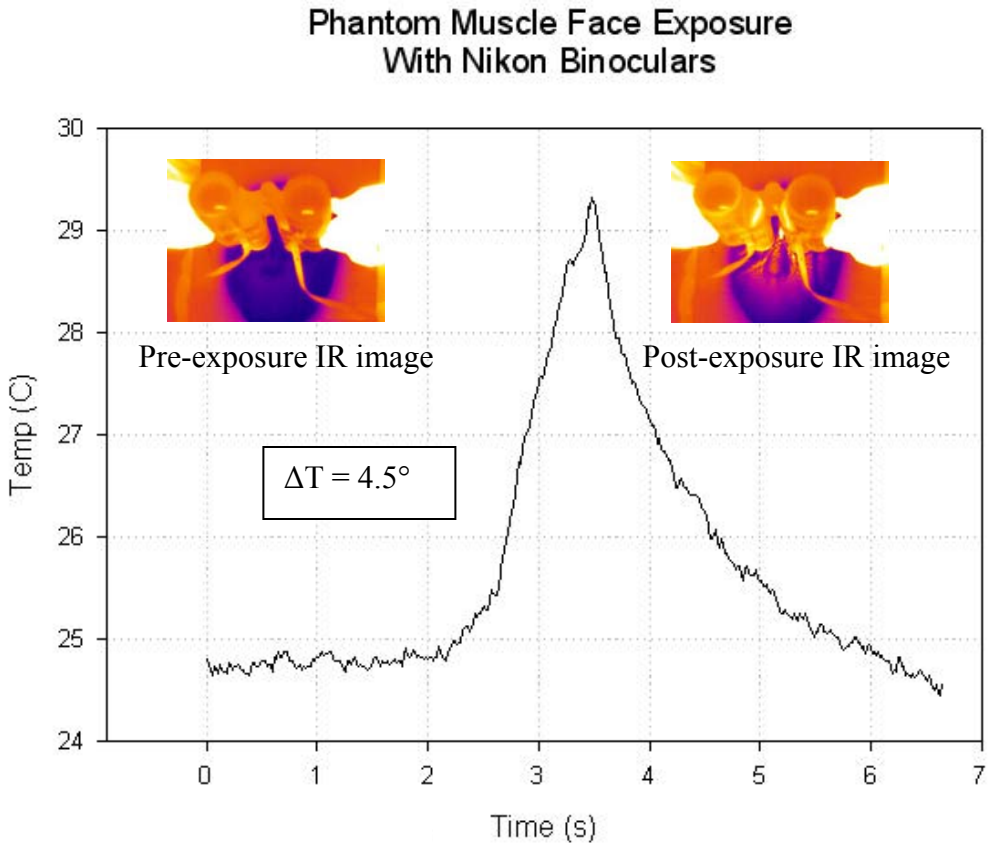

Figure 15. Temperature (C) rise on face (area of binoculars not included) during exposure as recorded by the FLIR S-60 infrared camera.

Beam Focusing

To determine if there is any focusing of the beam through the lens of the night-vision goggles and binoculars, measurements were recorded from the ocular area immediately following the removal of the goggles and binoculars at the end of each exposure period. A baseline was obtained using the temperature of an area located near the eyewear. Because the phantom material is homogeneous, the temperature of any area of the phantom face would be the same after a period of equilibration. Therefore, before an exposure, the temperature of the ocular area off the phantom face would be the same temperature of any other area. To be more accurate, the area recorded was exactly the same for both the baseline area (normally located on the forehead area directly above the ocular area) and the area of interest (ocular). Figure 16 and 17 show the results of this experiment. An exposed face wearing no eyewear is compared to a phantom face following the removal of night-vision goggles and binoculars. To look at the effects of the beam from different orientations, measurements were made at five different angles of incidence: 0°, 15° to the right and left of the beam, and 0° to the beam but 15° leaning forward and 15° leaning away, or backward, from the beam. In all cases, the area of the face between the eyes (bridge of nose) was located the same distance from the pyramidal horn antenna. The results are conclusive that there is no focusing of the beam through the lens of either the night-vision goggles or the binoculars.

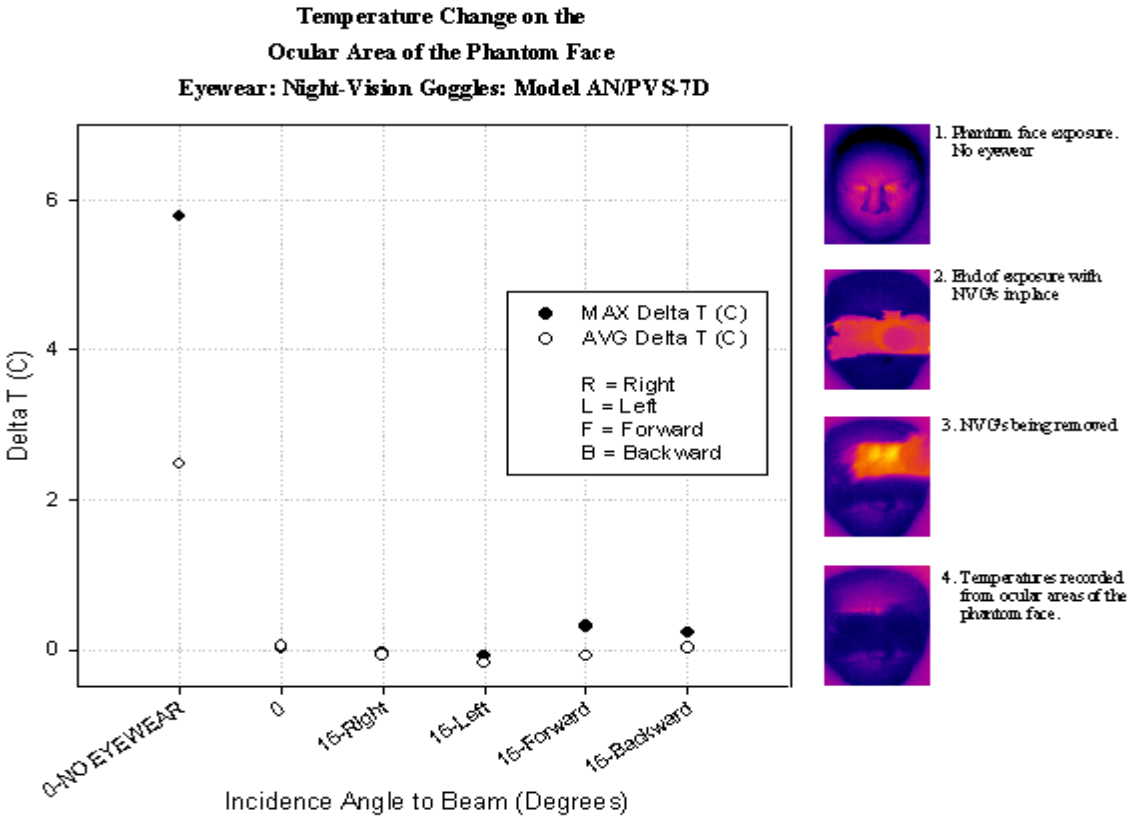

Figure 16. Comparison of heat deposited to the ocular area of the phantom face without eyewear and with night-vision goggles.

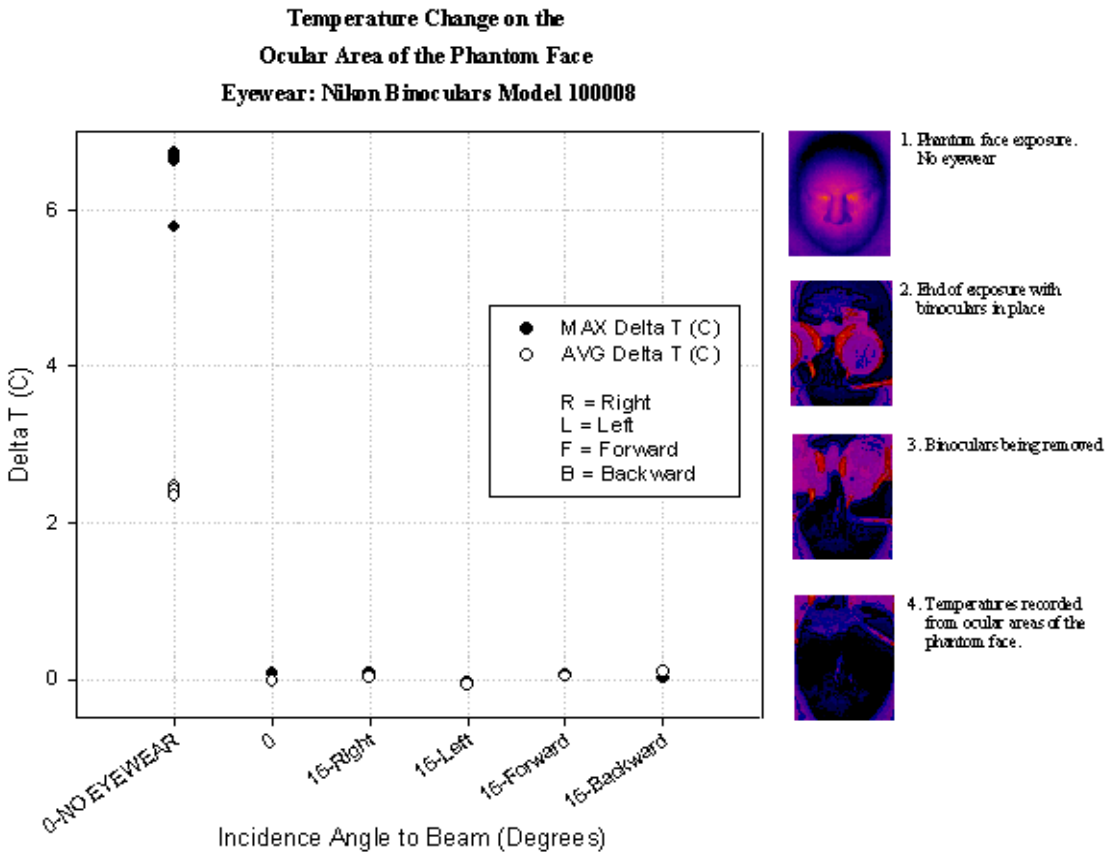

Figure 17. Comparison of heat deposited to the ocular area of the phantom face without eyewear and with binoculars.

Focusing of the beam on other areas of the face is also a concern. To determine if undesirable hotspots occur, data obtained from both the night-vision goggles and binoculars IR images were compared to data recorded from a phantom face wearing no eyewear. Figure 18 and 19 show the effect of the goggles and binoculars on the beam. The face with no eyewear clearly shows the hottest spots are located in the area located where the medial commissure (inner corner where eyelids join) of the human face is located. The hotspots, while wearing goggles or binoculars, are located on other areas of the face, however, these hotspots are not significantly higher than the temperatures measured on the phantom face wearing no eyewear. In each figure (18,19), the data point representing the hottest spot recorded is placed directly over the spot on the phantom face. Average delta T was calculated by taking the pre-exposure temperatures of entire area of the face, not including the eyewear, and subtracting that data from the same area temperatures following exposure. This data indicates that the overall temperature change is virtually the same with or without night-vision goggles or binoculars.

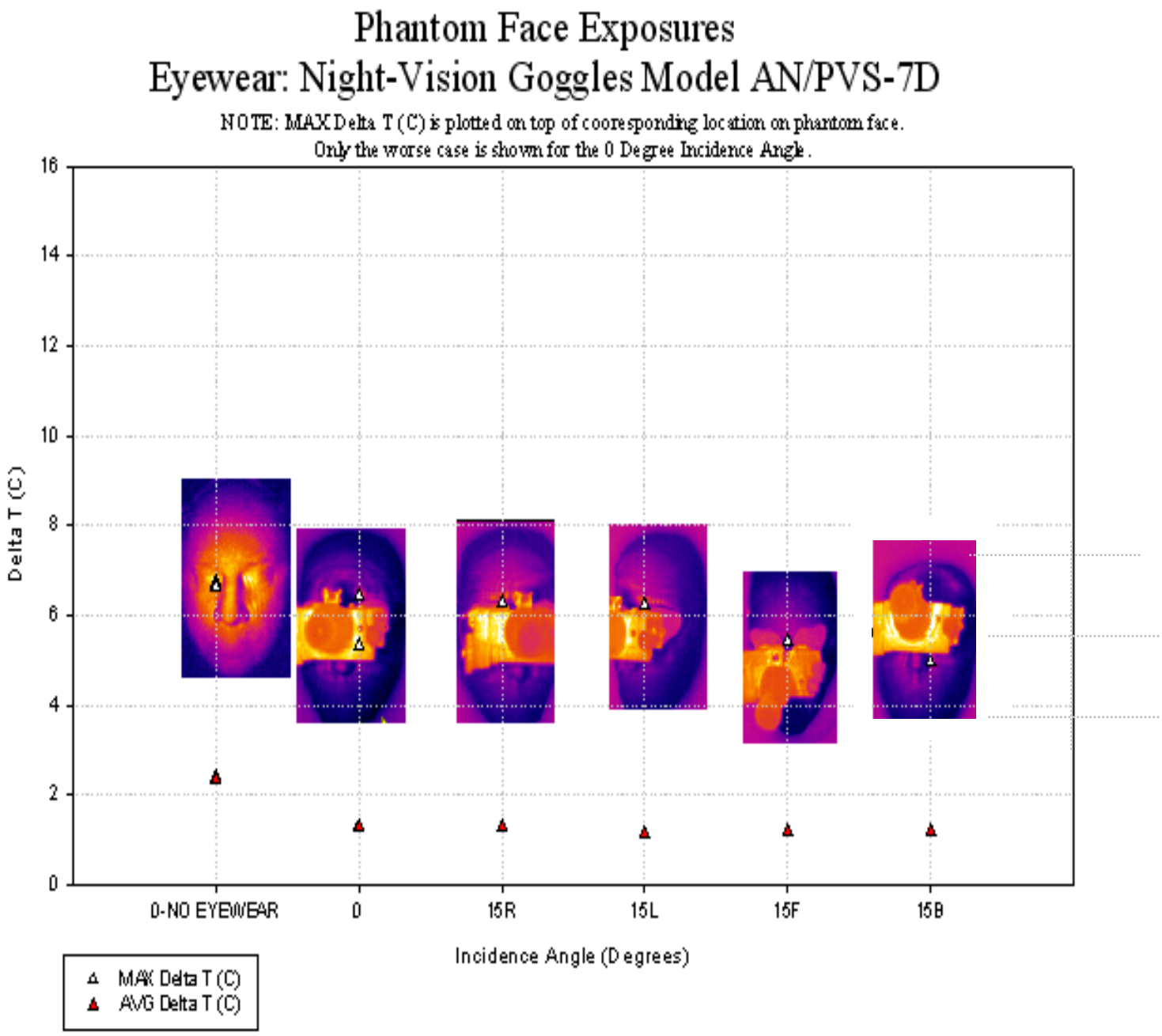

Figure 18. Hotspot comparison with and without night-vision goggles

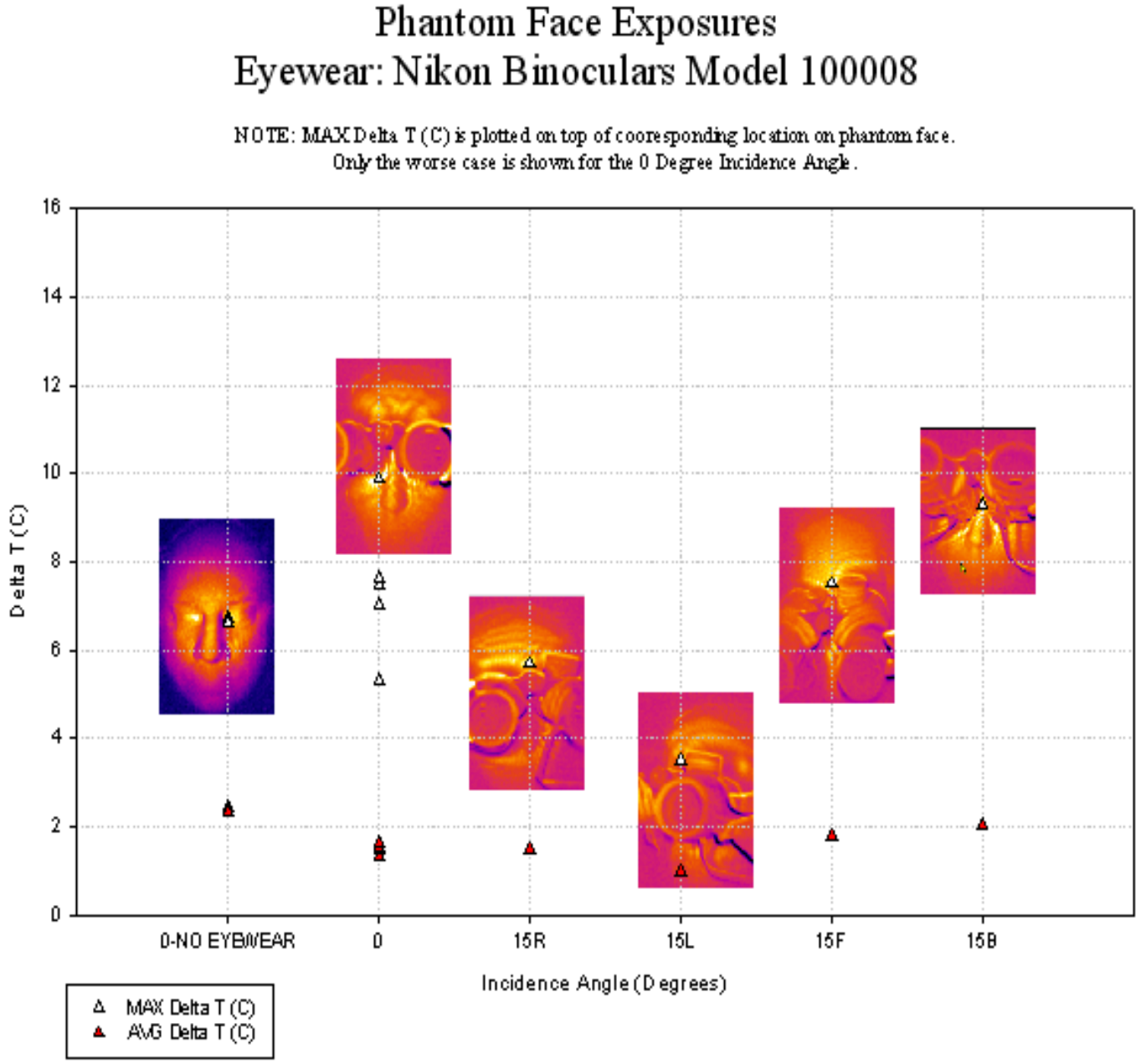

Figure 19. Hotspot comparison with and without binoculars

Conclusions

Although only one face shape is used as an illustration in this report, data from four dissimilar shaped phantom faces, with and without eyewear, was collected and included in the results. In addition, all four face shapes were irradiated at different angles of exposure to compare beam deflections caused by the shapes of the facial structures and eyewear. These evaluations show that all four face shapes affect the 94-GHz beam (deflections and reflections) somewhat differently; however, temperature rise, or hotspots, in all cases are very similar with no single exposure elevating to a level more than 10-degrees above pre-exposure values. Not one of the face shapes that were exposed showed any distinct focusing of the beam or hotspots caused by deflection of the beam any more than other faces that were compared. When wearing no eyewear, it was observed that in all cases the highest temperature increase was located in the inner canthus area of the eye of the phantom face. When wearing NVGs and binoculars, the hottest spots were located outside the area of the eye, normally on the forehead or nose area. Measurements were taken after both the NVGs and binoculars were removed from the face immediately after exposure and, as shown in graphs 5 and 6, indicate that the eyewear provides a layer of protection for the eyes. Temperatures measured in the areas around the eyes after exposure are well below the highest temperature on the phantom face and are near pre-exposure levels. There is no indication that the NVGs or binoculars focus the beam towards the area of the eye.

In every case, deflections of the 94-GHz beam occurred as did some focusing of the beam. However, these deflections and/or focusing did not cause a temperature increase at any particular location on the phantom face that would indicate the beam was focused enough to cause a damaging effect. The area or areas that were affected because of the eyewear had temperature increases that were very similar to the temperature increases occurring when no eyewear was worn. This suggests that eyewear, if worn while being exposed to the ADS operational parameters of exposure, will not cause damaging hotspots or aid in producing damaging hotspots on the surface of the face or eyes.

References

Chalfin S., D'Andrea J.A., Cox D., Crane C., Scribbick F. 94 GHz Energy Density for Irreversible Eye Damage in New Zealand White Rabbit Cornea (Oryctolagus Cuniculus). NHRC Technical Report-DEBL-2005-01. Naval Health Research Center Detachment Brooks City-Base, Brooks City-Base, TX 78235-5365

Chalfin S., D'Andrea, J. A., Comeau, P. D., Belt, M. E., and Hatcher, D. J. Millimeter Wave Absorption in the Nonhuman Primate Eye at 35 GHz and 94 GHz. *Health Physics*, 83:83-90. 2002.

Durney, C.H.; Johnson, C.C.; Barber, P.W.; Massoudi, H.; Iskander, M.F.; Lords, J.L.; Ryser, D.K.; Allen, S.J.; Mitchell, J.C. *Radio frequency radiation dosimetry handbook*. SAM-TR-78-22, Brooks Air Force Base, San Antonio, TX, 1978.

THIS PAGE INTENTIONALLY LEFT BLANK